Validation of AMSR-E Polar Ocean Products Using a Combination of Modeling and Field Observations

Annual Report
March 2004

James Maslanik[1], John Heinrichs[2], Thorsten Markus[3], Julienne Stroeve[4], Matthew Sturm[5]
(with contributions from Dylan Powell[6] and Don Cavalieri[3])

[1] University of Colorado, CCAR, Boulder, CO
[2]Ft. Hays State University, Fort Hays, KS
[3]NASA-Goddard Space Flight Center, Greenbelt, MD
[4]CIRES, University of Colorado, Boulder, CO
[5]U.S. Army Cold Regions Research & Engineering Laboratory-Alaska, Fairbanks, AK

Contact: james.Maslanik@colorado.edu
303-492-8974

Table of Contents

(Cover photo: NASA P-3 overflying Barrow-area field transects at 500ft. altitude, 13 March 2003.

1.0 Project Overview

The goal of this effort is to complement and enhance the EOS Science Team's AMSR validation plan by combining additional detailed, *in situ* data collection with radiance modeling to evaluate products under a variety of weather and surface conditions. This report describes activities during Year 2 of the project and planned activities for Year 3. Section 1 provides background and an executive summary, Section 2 reviews the main activities associated with the "AMSRIce03" field campaign, Section 3 presents results of modeling activities, Section 4 highlights data assembly and analysis, and Section 5 describes activities anticipated in Year 3.

1.1 Background

As we note in the following sections, the main premise of our approach is that, for most sea ice conditions, it is impractical to collect certain critical types of *in situ* data at sufficient spatial and temporal detail to serve as direct validation of satellite-derived products. Specifically, snow depth and snow characteristics, snow/ice column temperatures, surface roughness, and ice thickness and ice characteristics vary over small scales as well as large, and in some cases vary rapidly over time. At present, these parameters require direct measurement from the surface. The nature of sea ice as well as logistics, safety, cost and availability of trained personnel limit the extent of the areas that can be sampled in sufficient detail even over the most benign ice conditions. Thus, detailed sampling of ice and snow for validation over distances representative of even a single AMSR-E pixel is, in practice, not achievable without a massive commitment of people and resources.

With this in mind, the linchpin of our strategy is to use aircraft measurements to bridge the "spatial sampling gap" between surface measurements and satellite products, both for direct evaluation and through modeling. This is being done in several steps, following two paths of investigation. The first path is an empirical one: We select field locations that provide as varied an ice cover as possible (to represent a range of ice conditions) but with spatial variability that is of sufficiently large scale to reduce within-pixel variability to an acceptable level in passive microwave pixels acquired by aircraft (in this case, the Polarimetric Scanning Radiometer [PSR] onboard the NASA P-3). Second, we then use the *in situ* measurements to interpret the aircraft microwave data and to evaluate accuracy of AMSR-E algorithms applied to the aircraft imagery. Third, the aircraft data provide the means of mapping the surface over areas large enough to be directly comparable to AMSR-E pixels.

The second path makes use of modeling to allow us to extend our validations to conditions not included in the direct measurements, to better assess the physical properties that contribute to algorithm error, and to test relationships among micro-scale conditions (such as snow grain size) and larger scale properties (such as smooth vs. rough ice) that could be used to improve algorithm performance by constraining error associated with the micro-scale properties. To support this line of investigation, we need to collect additional snow, ice and atmospheric data that are needed as model input –

again over scales representative of PSR pixels. We then test the models using these inputs, with the aircraft microwave imagery providing the "model validation" data sets. The models are refined based on these comparisons and then used in sensitivity studies to quantify the effects of various conditions on algorithm performance over satellite scales.

As the above summary suggests, the key data requirements of our project are that we collect *in situ* data over scales useful for comparison to aircraft data, that these data as much as possible include the full range of parameters that substantially influence the microwave signal from sea ice, that the aircraft acquires its data sets precisely over the same areas sampled on the surface, and that the surface and aircraft operations be conducted coincident in time. The resulting combined surface/aircraft campaign ("AMSRIce03") that we planned and carried out to achieve these objectives is summarized in Section 2 and in more detail in Appendix 1.

1.2 Summary of Year 2 Activities

Key activities during Year 2 include:

- Successful completion of the AMSRIce03 field campaign, including extensive *in-situ* data collection and coordinated aircraft overflights in the Barrow, AK area and at an ice camp in the central Beaufort Sea.
- Summary and initial analyses of the AMSRIce03 data sets.
- Acquisition and georeferencing of ancillary satellite imagery.
- Model sensitivity studies involving the MWMOD sea ice/atmosphere model and the MEMLS snow model, including indirect coupling of these models to describe the complete ice/snow/atmosphere column.
- Integration of the AMSRIce03 field data with model calculations for direct comparison to PSR imagery acquired by the NASA P-3.

Key results and findings include:

- Coincident sampling and characterization of sea ice and snow cover; allowing development of basic relationships between ice roughness and snow depth to an extent that has likely never before been achieved in a combined field/aircraft campaign.
- Calculations using MEMLS demonstrate the sensitivity of microwave emission over sea ice to snowpack properties – particularly depth and grain correlation length (a measure of grain size and shape).
- Comparisons of PSR imagery to in-situ snow and ice observations confirm our ability to georeference the aircraft data to the detailed surface transects, and confirm that we can bridge the difference in scales between the surface and aircraft observations – a critical requirement for our research approach.
- Comparison of in-situ measurements, PSR imagery and microwave modeling demonstrate the capability of the microwave models to reasonably reproduce the aircraft PSR measurements when supplied with surface data as model input – a second critical requirement of our approach.

2.0 AMSRIce03 Field Campaign Overview

(An overview of the 2003 field effort is given here. Please see Appendix 1 for a detailed report on the field activities.)

The joint *in situ* and aircraft campaign, referred to as "AMSRIce03", was conducted over a 3-week period in March 2003. This field experiment consisted of an extensive set of surface measurements over sea ice, coincident with overpasses of the NASA P-3 aircraft (Figures 1 and 2) at the Barrow area (Figure 2) on 13 March 2003 and 19 March 2003, with aerial photograph mapping by single engine aircraft and an small unmanned aerial vehicle (an "Aerosonde" UAV) and at a U.S. Navy ice camp in the central Beaufort Sea (Figures 3 and 4) on 19 March 2003. (Note: this summary addresses only the joint surface/aircraft campaign – for information on the overall P-3 flight operations, which included flights over other areas without coincident field measurements, please see the companion AMSR validation report submitted by D. Cavalieri, et al.).

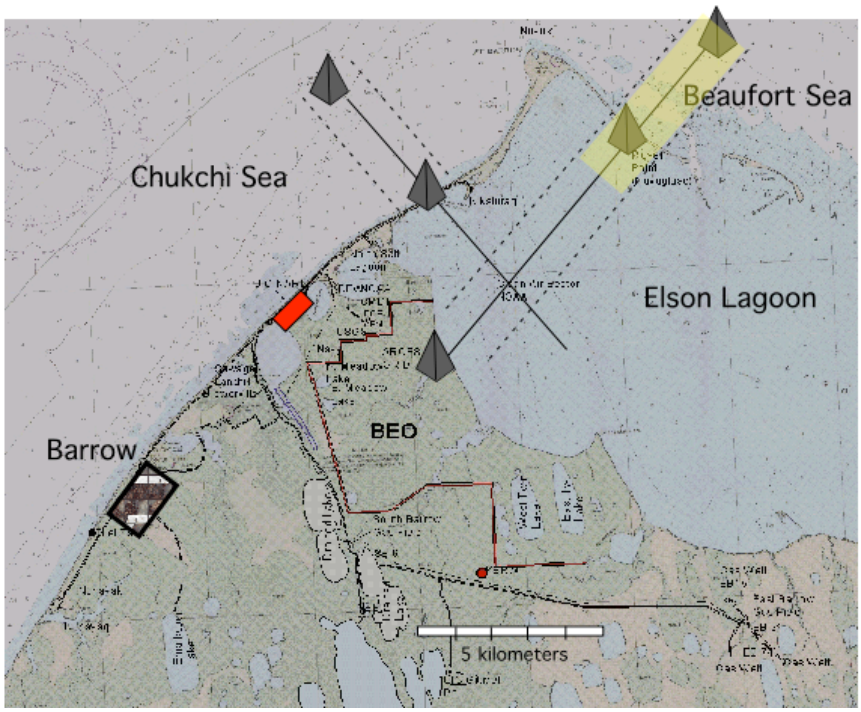

Figure 1. Barrow area map showing the Chukchi, Beaufort and Elson measurement areas and the two intersecting traverse lines, as well as the approximate swath (dashed lines) of aerial photography. The yellow area indicates the coverage of the example photo-mosaic shown in Figure 5.

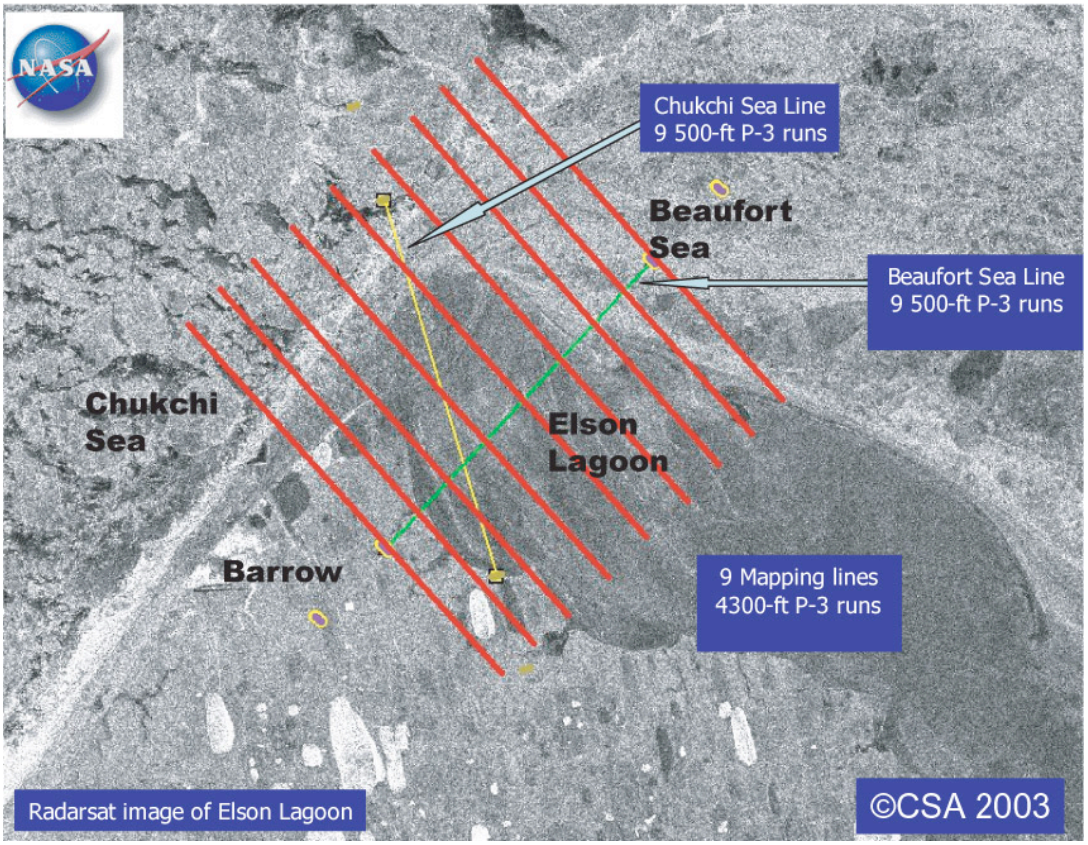

Figure 2. Site map of the Barrow study area. Place names, surface transects and NASA P-3 aircraft flight lines are shown superimposed on a RADARSAT synthetic aperture radar image. The Elson transect is shown in green. The Chukchi transect is shown in yellow. Note the relatively even texture of the Elson Lagoon ice (indicating relatively smooth ice) compared to the variability in ice conditions apparent along the Chukchi Sea coastline and offshore of the barrier islands enclosing Elson Lagoon to the north.

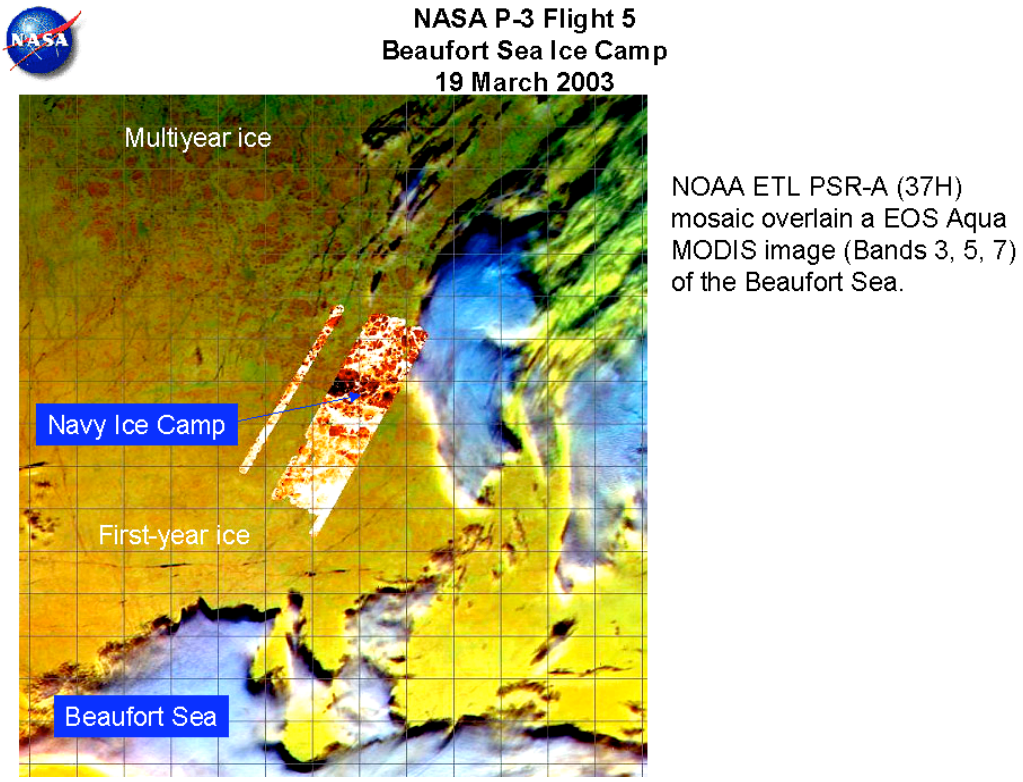

Figure 3. Composite of P-3 PSR data and MODIS imagery, depicting the location of the U.S. Navy ice camp (the "Ice Camp" site).

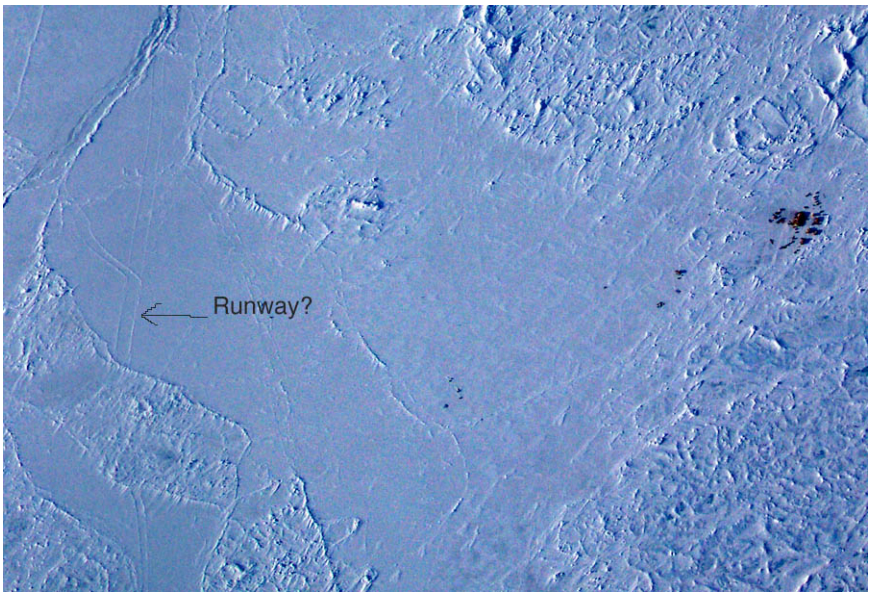

Figure 4. Subsection of a mosaic of P-3 digital photographs over the Ice Camp study area. In this example, the camp is visible on the right side of the image. The camp's runway is indicated on the left.

The in-situ field effort had four main objectives:
(1) Sample those parameters that are most relevant for microwave emission and remote sensing of sea ice;
(2) Measure these parameters over space and time scales sufficiently large and detailed to permit direct comparison to aircraft microwave imagery and AMSR-E proxy (aircraft-derived) products generated using the standard AMSR-E algorithms;
(3) Collect these and additional data sets at suitable space scales needed to test and validate microwave emission models using aircraft PSR data for comparison;
(4) Collect data sets in such a manner that it becomes possible to investigate relationships between micro-scale conditions and larger conditions, with the intent of providing information applicable to reducing algorithm errors associated with variations in small-scale properties.

The two study areas provided access to a range of sea ice conditions as shown earlier in Figure 2 – smooth, rubbled, lightly ridged and heavily ridged first-year ice, multiyear ice with refrozen ponds, and ice of various thicknesses. (For additional images of ice characteristics and other project photos, please go to http://polarbear.colorado.edu/AMSRICE/AMSRIce03.html.) The bulk of the measurements were collected over shore-fast ice near Barrow, but the inclusion of sampling at the Navy ice camp provided access to pack ice made up of of first-year and multiyear floes. Weather conditions during the period consisted of relatively high winds and blowing snow during the first several days, following by predominantly clear skies or thin cirrus with light to moderate winds over most of the remainder of the days. Air temperatures ranged from mid-day temperatures of about –15 C early in the study period to about –30 C at the end of the field campaign (Figure 5).

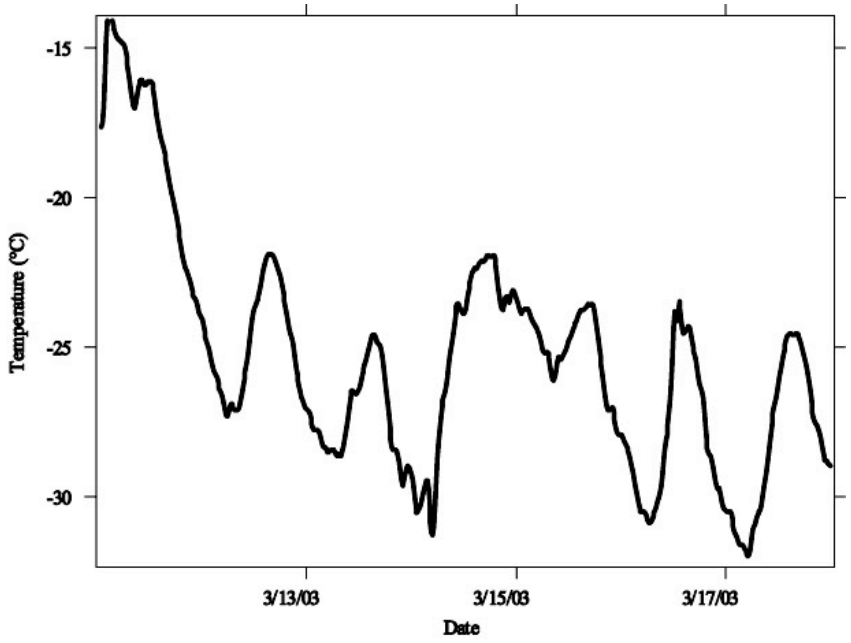

Figure 5. Surface air temperatures (at approximately 1m height) during the Barrow study period, recorded over shorefast ice near Barrow.

Most of the *in situ* measurements were collected along transects (see Figure 1), referred to as the "Chukchi Line" and the "Elson Line" at the Barrow site, reflecting the locations of these transects on the Chukchi Sea coast and crossing Elson Lagoon, respectively. The Chukchi Line spanned an area of relatively smooth ice, beginning on the western end of Elson Lagoon, progressing west-northwest toward ice of increasing roughness, ending within an area of ridged ice. The Elson Line extended from just inland of Elson Lagoon, crossing the smooth ice of Elson Lagoon to the north-northeast (Figure 6), across barrier islands near Plover Point, and extending over heavily rubbled and increasingly ridged ice at the northern end of the transect. Together, the two lines covered over 20km.

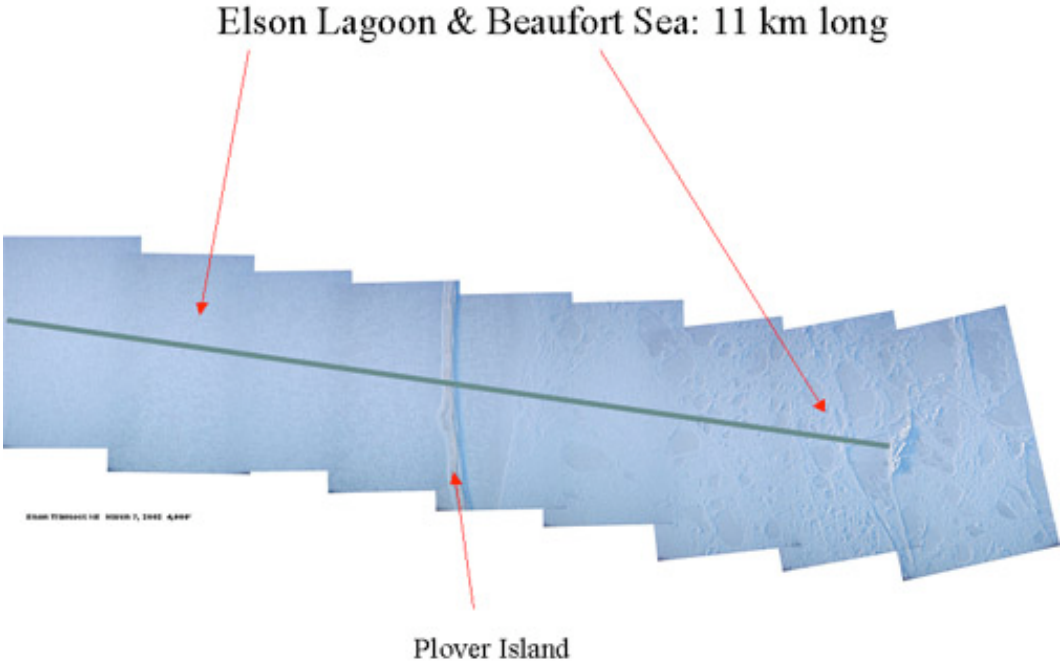

Figure 6. The Elson Line, shown superimposed on a mosaic of high-resolution aerial photographs acquired by the Cessna 185.

Both transects were surveyed to centimeter accuracy using a Trimble GPS unit, receiving transmission from the GPS base station at the UIC-NARL building in the UIC-NARL complex. Surveyed positions along the transects were marked with stakes at 100m intervals. To provide markers visible to the Cessna and P-3 pilots, the two end locations of each transect were marked with black "targets" formed from road-bed cloth (a low-cost and durable material) draped and stapled over a tripod of 2x4s. Each target was approximately 2m in width and 9m tall. The targets proved surprisingly resistant to strong winds and remained in place during the entire campaign, although the northernmost Elson Line target required repairs following its investigation by polar bear(s). As with all other items placed on the ice, the targets were removed at the end of the experiment.

To achieve our goal of collecting field data that sufficiently lined up with and represented the microwave data acquired by the PSR on the P-3 required that the P-3 overfly our surface transects with no more than a 200 to 300m alignment error at a flight altitude of 500ft. This introduced several critical elements to the project. First, we needed precise geolocation of the surface transects. Second, the P-3 needed sufficient onboard navigation capability to achieve the required geolocation accuracy (and/or the ability of the pilots to locate and follow the transect lines by eye. The added complication of ice drift made this alignment even more difficult for the Ice Camp site.) Third, the transect GPS coordinates and resulting flight lines had to be delivered to, and adhered to by, the aircraft crew and onboard scientists. Fourth, the field crew needed to be in place on the ice and engaged in sampling of the most time-sensitive parameters (skin and subsurface temperatures in particular) during the times of overflights (Figure 7).

Figure 7. Photograph illustrating the close coordination achieved between the NASA P-3 (shown flying overhead), the surface transects and the field crew. In this case, the hut and crew member are positioned at the intersection of the Chukchi and Elson lines (with other crew members elsewhere along both transects). This allowed us to verify the flight tracks of the P-3.

This close coordination in time and space between a surface crew and a large research aircraft is a highly unusual requirement but was critical to our project goal of linking *in situ* measurements (representing detailed but local scale observations) with the broader scale "AMSR-E simulator" data acquired by the P-3. The coordination was successfully achieved thanks to the skill and cooperativeness of the aircraft operations crew, staff and scientists and the diligence of the *in situ* field crew.

With the exception of new and young ice, which were sampled from aircraft but not with in-situ measurements at the Elson and Ice Camp sites, observations included coincident measurements of:

- ice thickness (drilling and electromagnetic inductance [EM-31]),
- ice type (general categories)
- ice roughness,
- ice salinity, brine and bubble volume,
- snow properties (depth, density, layering, grain size, grain type, snow water equivalent),
- skin temperature,
- snow/ice interface temperature,
- temperature within the ice column,
- microwave brightness temperatures at 91 GHz.

Examples of data collection are shown in Figures 8a-d.

Figure 8a. Collection of various snow and ice parameters during AMSRIce03.

In addition to the extent to which AMSRIce03 yields combined surface and aircraft data, a unique aspect of the *in situ* measurements during AMSRIce03 is the relatively fine

spatial detail sampled, compared to previous field efforts. Figures 9a-d depict this level of detail embodied in the snow depth and ice thickness measurements.

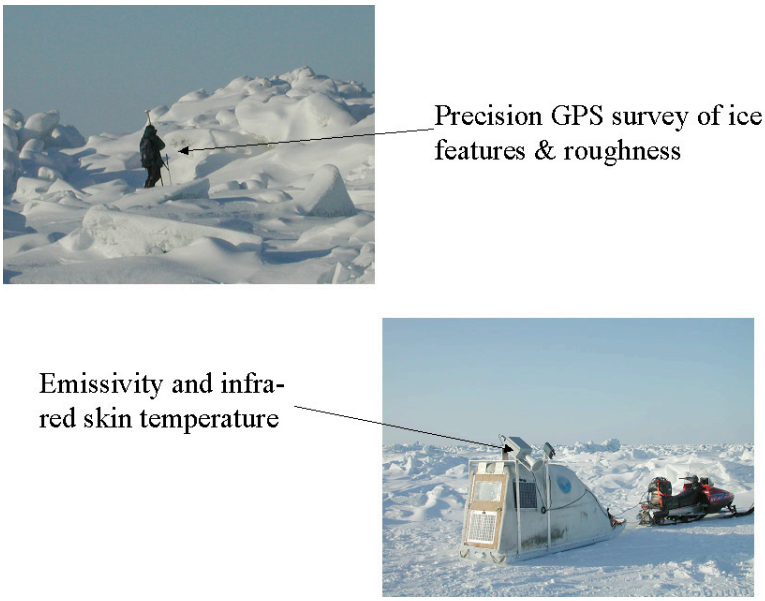

Figure 8b. Collection of various snow and ice parameters during AMSRIce03.

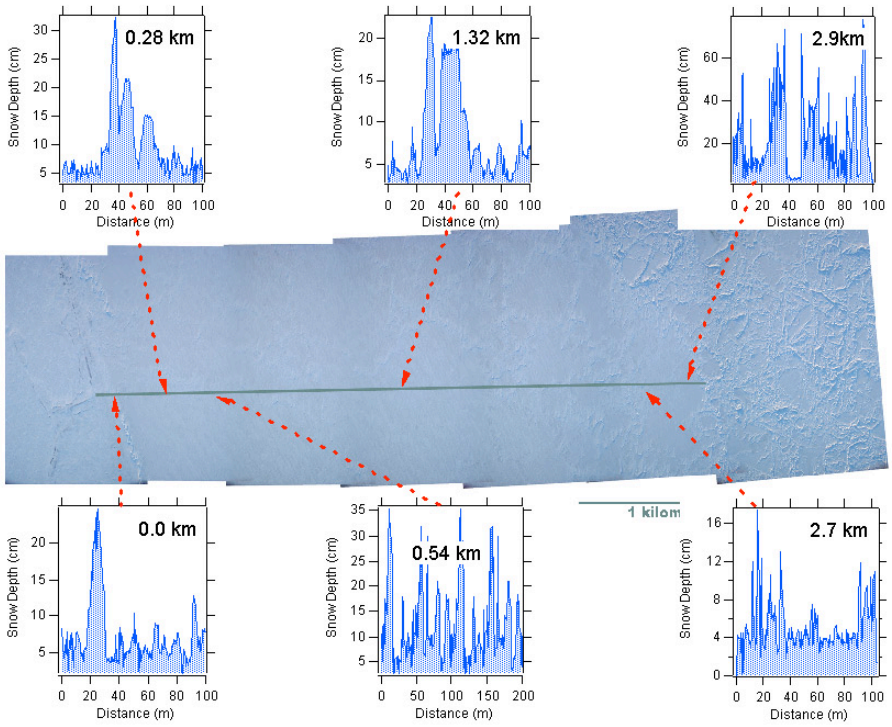

Figure 9a. Samples of snow depths collected along the Chukchi Line, showing the degree of detail contained in the *in situ* data sets.

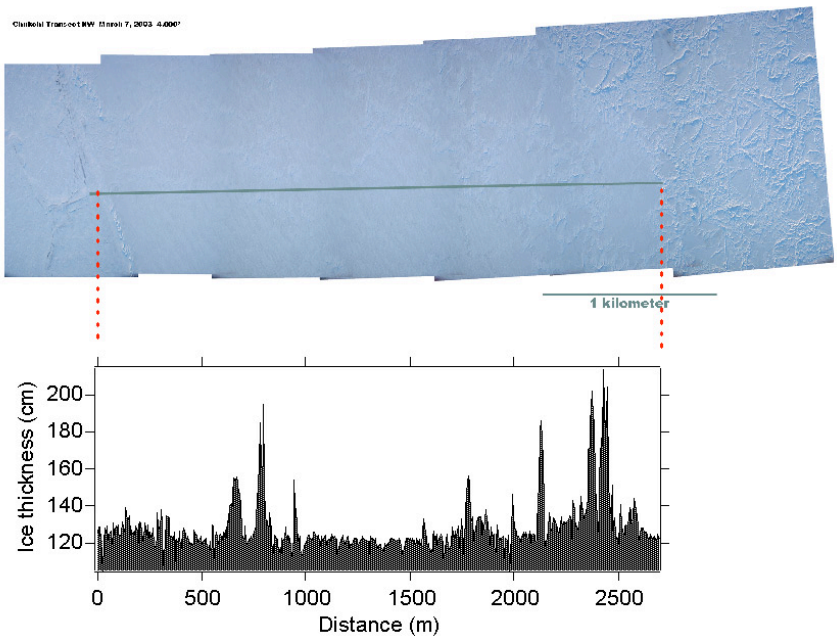

Figure 9b. Ice thickness measured along the Chukchi Line using the EM-31.

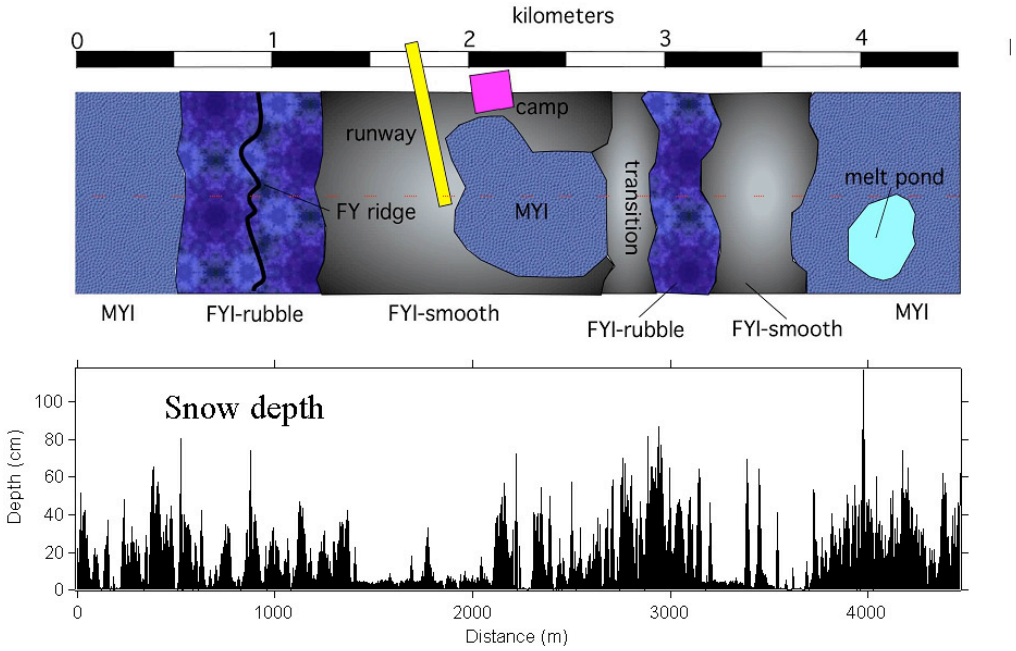

Figure 9c. Sketch of ice conditions and corresponding measurements of snow depth along the Ice Camp Line. Note the correspondence between less snow on the relatively young first-year ice (FYI) and the rougher rubbled first-year and multiyear (MYI) ice.

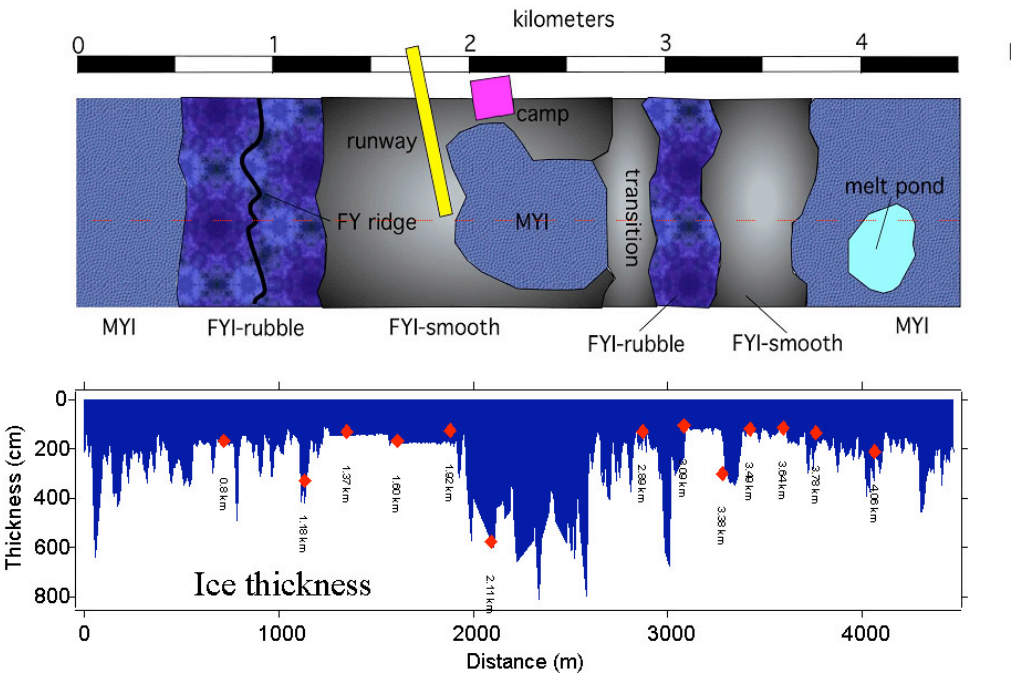

Example 9d. Sketch of ice conditions and corresponding measurements of ice thickness along the Ice Camp Line. Notice the correspondence of ice thickness with the general ice categories such as the smooth (and thinner) first-year ice and the thick multiyear floe in the center of the line.

The measurement methods included the following (see Appendix 1 for details): For snow depth, "Magnaprobe™" devices were used to record snow depths at spacings of approximately 1 to 2m along the entire lengths of the Elson and Chukchi transects and along the perpendicular transects. Large-scale height and roughness (including finely spaced measurements over snow dunes and rubble and at larger spacing over ridges) were measurement using the Trimble survey-grade GPS unit with real-time or post-processed differential GPS positioning. Additional small-scale relief was recorded using a laser survey system.

To supplement the transects and provide data for assessing the spatial representativeness of the lines (particularly in the event of misalignment between the aircraft and ground tracks), shorter tracks oriented perpendicular to the main transect lines were also sampled. In addition, other areas of the ice cover were investigated and mapped using roving GPS survey units carried on foot and on snowmobiles. Skin temperature and brightness temperatures at 91 GHz were collected along the Elson and Chukchi lines using at Heimann KT-19 and a passive microwave radiometer mounted on a sled (shown deployed in Figure 8b) and towed by snowmobile.

Data collected by the NASA P-3 during its overflights included PSR data (PSR-A and PSR-CX subsystems, with the PSR operated in scanning mode during the 5000 ft. flight tracks and in staring mode (looking directly forward in the along-track direction) during

the 500 ft. flight tracks), the NASA Airborne Topographic Mapper (ATM) scanning laser, digital and video cameras and an infrared imager.

In addition to these spatially distributed measurements, four stations were deployed that included continuous measurement of temperatures within the ice and snow column as well as air temperatures. Basic atmospheric column data were obtained from the existing Dept. of Energy Atmospheric Radiation Monitoring (ARM) site and the NOAA Climate Modeling and Diagnostics Laboratory (CMDL) facility, both of which are located within 10km of the Barrow field area, and rawinsonde launches from the ARM site and the National Weather Service office in the town of Barrow (about 6km south-southeast of the field measurement locations).

2.1 AMSRIce03 Results

Here, we illustrate some of the results to date from analyses of the *in situ* data. For more information, please see Appendix 1. Much of our initial work with these data has emphasized the retrieval of basic relationships between key snow and ice parameters. These relationships can then be use to assess performance of the AMSR algorithms over other sea ice areas, including providing for the possibility of "confidence flags" for different locations and conditions. In addition, these relationships provide fundamental knowledge about the physical properties of the ice pack. These can then form the basis for future algorithm improvements and extensions and provide information for refining sea ice models. Below, we note results for two of these basic relationships – snow depth vs. ice temperature, and snow depth vs. ice roughness and thickness.

Validation of AMSR-E's "sea ice temperature" product required collection of temperatures at various levels within the snow/ice column. In general though, over relatively thick first-year ice, the effects of brine inclusions means that the AMSR-derived ice temperature will most closely correspond to the temperature at the snow/ice interface. One of the main controls on snow/ice interface temperature is snow depth. Figure 10 shows the relationship between snow/ice interface temperature and snow depth for different field locations during AMSRIce03.

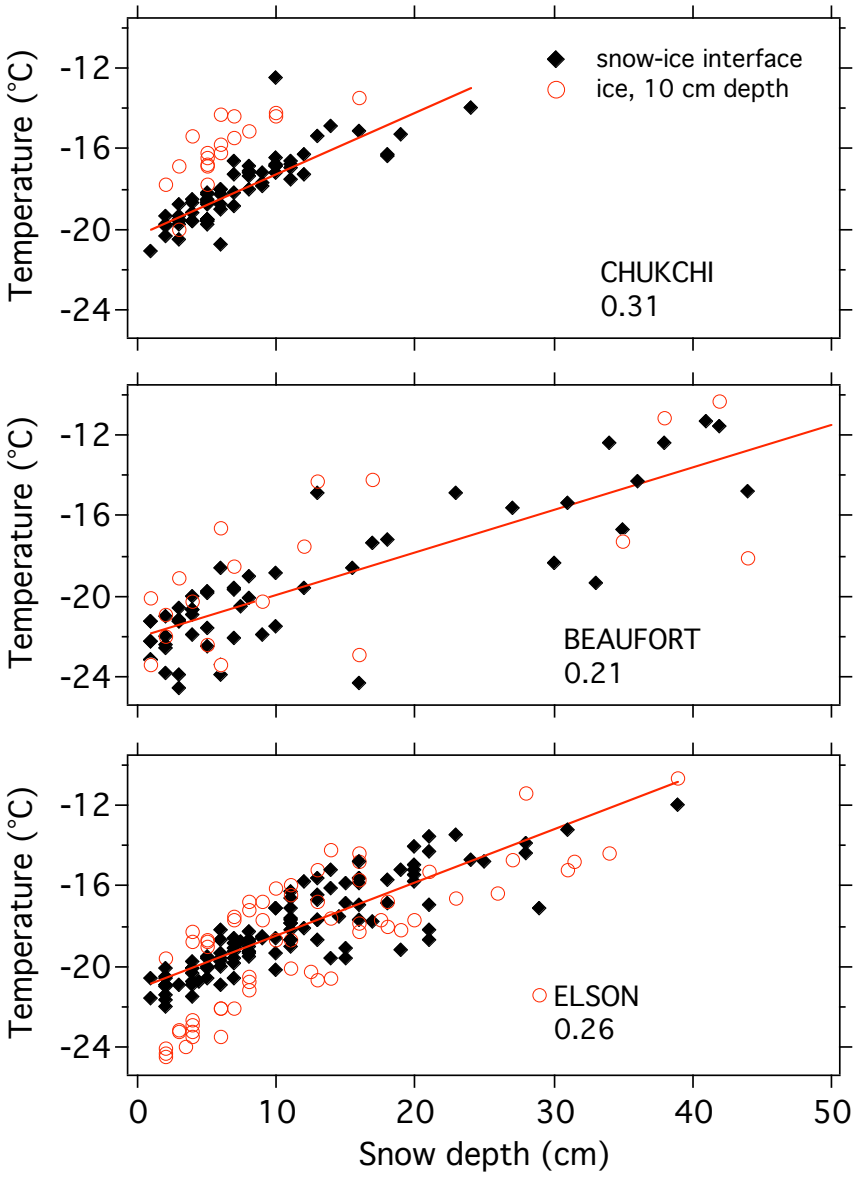

Figure 10. Snow-ice interface temperatures, and ice temperatures (at 10cm depth) as a function of local snow depth for the three Barrow field areas. The number beneath the area name is the slope of the best fit line to the snow/ice interface temperature.

Snow depth over sea ice is affected by several ice-related factors – age of the ice (i.e., length of time that the ice is present to accumulate snow), orientation of ridges relative to wind direction, and variations in surface roughness. For the latter factor, insufficient concurrent data on snow depth and ice thickness and roughness have been available to attempt to reliably quantify relationships between snow depth and ice conditions. The AMSRIce03 effort provides such data, and even in early analyses is providing some strong evidence about the controls of ice roughness on snow accumulation and capture. Figure 11 shows some fairly typical results where snow depth correlates well with ice thickness.

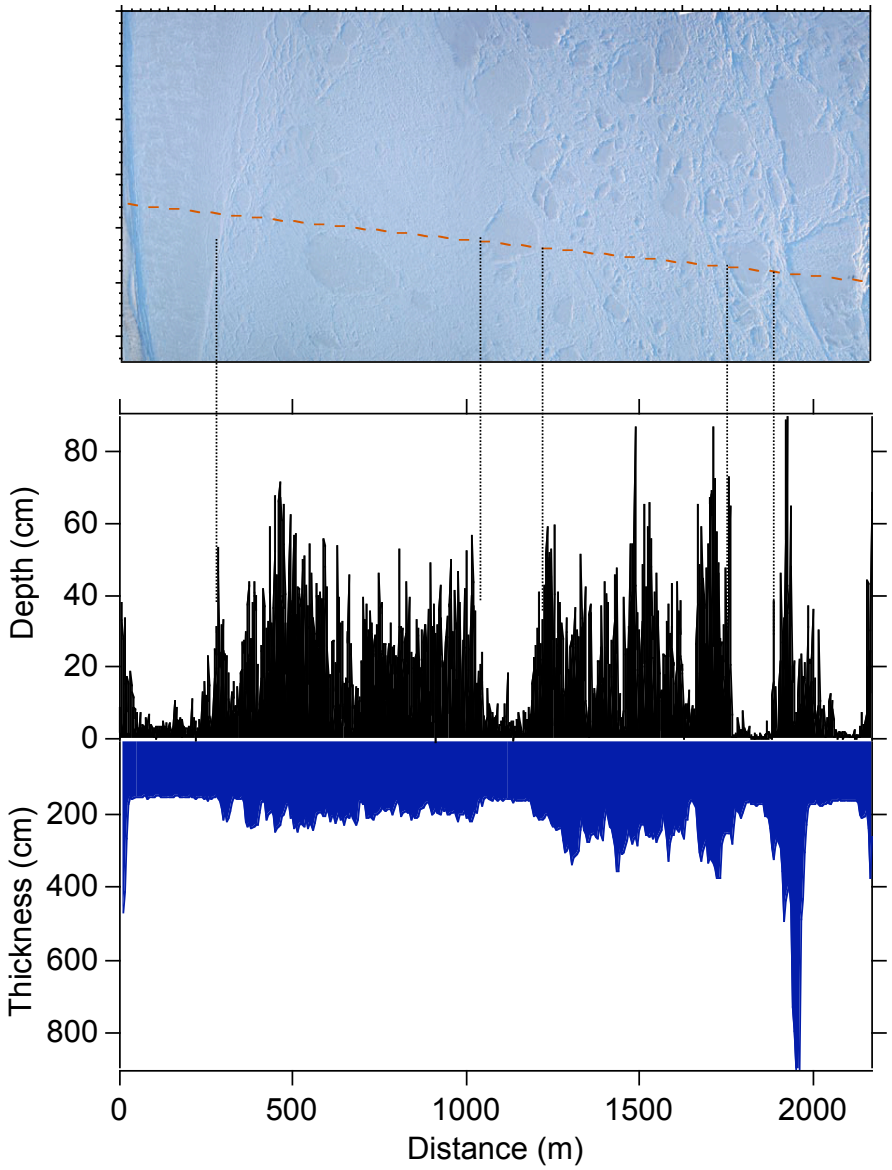

Figure 11. Ice thickness and snow depth along the main transect line, Beaufort Sea, showing a striking correlation between the two variables. Undeformed floes (with thin ice and snow) surrounded by deformed ice and rubble fields can be seen in the photo-mosaic (top panel).

2.2 Comparisons of *In situ* Data with Aircraft Data

The PSR data have only recently been delivered by NOAA for the Ice Camp flights and have not yet been delivered for the Barrow flights. The Ice Camp PSR data are not fully calibrated, but nevertheless we have been able to begin some fruitful comparisons between the surface observations and PSR microwave brightness temperatures. Figure 12 illustrates such a comparison, showing gradient ratio calculated from the PSR data

compared to snow depth along a portion of the Ice Camp line. The results reveal correspondence between the gradient ratio variability and snow thickness, as one would expect if we were sampling sufficiently large areas on the surface. Such comparisons establish a key project element of being able to associate surface conditions with the PSR data acquired from aircraft. We are still addressing issues of precise geolocation in this case due to uncertainty introduced by the drift of the pack ice, but initial results suggest that we can achieve good geolocation through a slight correction in positioning to account for drift of the ice camp between the time when the *in situ* data were collected and the time of the P-3 overflights.

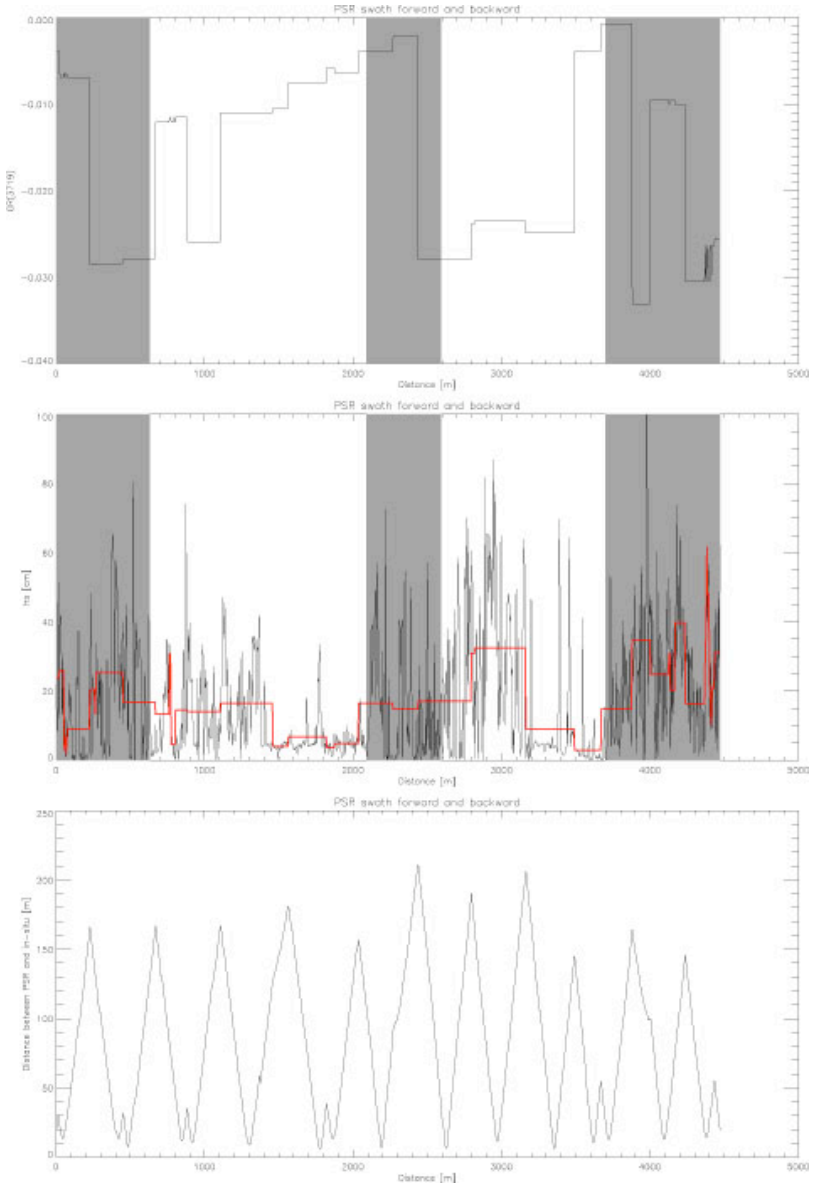

Figure 12. Intercomparison of aircraft-acquired PSR results with snow depth along a portion of the Ice Camp line.

2.3 AMSRIce03 Summary

From our analyses to date, we can conclude that the data collected during the AMSR-E calibration/validation campaign near and off-shore of Barrow, Alaska are extensive and cover most aspects of the snow and ice environment. These data, along with the close coordination achieved with the P-3 overflights, indicate that the field effort met the main objectives outlined earlier.

Additional samples of the *in situ* data are presented in Appendix 1. These data are in the process of being archived and documented, and in addition to supporting our validation effort, we expect that the data sets will provide an excellent "legacy" in the form of a general description of what the ice and snow conditions are like for arctic sea ice.

The data reinforce a well known fact: the snow and ice environment of arctic sea ice is extremely heterogeneous. This heterogeneity extends from ice thickness and snow depth to physical temperature, grain size, snow water equivalent and roughness. In many cases, the spatial scale of the variability is less than 10-m, and only for a few attributes does the scale extend to hundreds of meters (e.g., note the limited range in the various semivariograms presented in this report). One impact from this heterogeneity is that all pixels, satellite or aircraft, are "mixed" – more or less so, depending on the parameter in question. The fact that meaningful retrievals can be made from the remote sensing data implies that (fortunately), properties related to the remote sensing tend to aggregate around mean values, which should allow us to meet one of our key objectives of minimizing within-pixel variability in the PSR data, such that we can interpret the relationships between surface conditions and the PSR brightness temperatures.

One surprising finding from the field data was that the snow and ice conditions in the Beaufort Sea, just a few kilometers off the land, were similar to the conditions at the Navy Ice Camp, hundreds of kilometers off-shore. This similarity existed, despite the fact that the near-shore Beaufort ice was first-year ice while the off-shore Beaufort ice was mixed multiyear and first-year ice. We attribute this similarity to the fact that roughness, not age of the ice, was the controlling variable, with the degree of deformation the critical factor. Thus, the near- and off-shore Beaufort ice had similar roughness, this led to similar snow-holding capacity, similar temperature conditions and so on. An implication of this finding is that it is reasonable to conduct calibration/validation campaigns near Barrow, where the costs are considerably less than those incurred conducting similar tests well off-shore.

3.0 Modeling Activities

Modeling activities during Year 2 focused primarily on testing of the Microwave Emission Model of Layered Snowpacks (MEMLS) (Wiesmann and Maetzler, 1999), {Maetzler and Wiesmann, 1999) and MicroWave MODel (MWMOD) (Fuhrhop et al.,1997) for applications over sea ice. MEMLS is a thermal microwave emission model and is based on radiative transfer, taking multiple volume scattering and absorption into account. Since microwave scattering efficiency depends upon snow pack properties, the model accounts for the sensitive parameters such as grain size, density, temperature, and liquid water content. MWMOD is an emission model developed for use with a layered sea ice column, single-layer snow cover, and includes an atmosphere model.

The goal in using these two models is to combine the sophisticated multiplayer snow treatment of MEMLS (written as Matlab code) with the detailed ice simulations of MWMOD (written in Fortran). We investigated the possibility of recoding the models to physically merge the software into a single, combined snow/ice/atmosphere model but decided that the programming and testing effort was beyond the scope of our validation project. Instead, we concluded that we could achieve similar performance using an indirect coupling approach (Figure 13). In this approach, MWMOD is run to provide emissivities at the snow/ice interface. These emissivities are then supplied to MEMLS to provide emission to the lowest snow layer (equivalent to prescribing "ground" emissivities in MEMLS). Finally, the resulting snow surface emission is used as surface emission input into MWMOD's atmosphere model or other microwave atmosphere models.

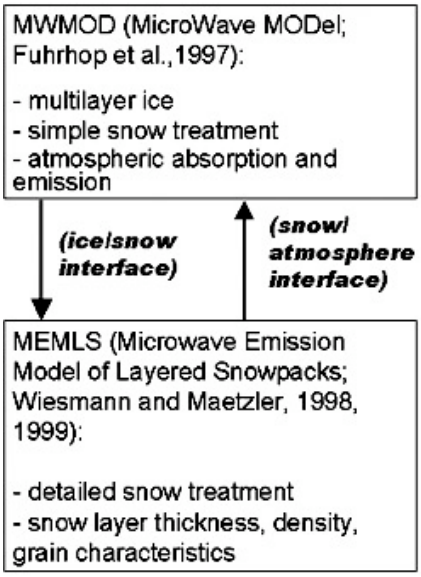

Figure 13. Relationships between the two microwave emission models currently being used in our project to simulate snow/ice/atmosphere brightness temperatures.

The bulk of the modeling work during Year 2 pertained to (1) testing the sensitivity of the AMSR-E snow depth algorithm to snow conditions, and (2) comparing simulations to data collected during the AMSRIce03 campaign. The snow depth retrieval algorithm used for AMSR-E (Markus and Cavalieri, 1998) is based upon the different scattering efficiencies of snow particles at 19 and 37 GHz. Brightness temperature at both polarizations decreases approximately linearly with increasing snow depth. The effect of scattering decreases with increasing wavelength. Thus, brightness temperatures at 37 GHz are reduced more than brightness temperatures at 19 GHz with increasing snow depth. Generally, the greater the difference, the greater the snow volume assumed to be present.

Unfortunately, snow pack properties can greatly alter the scattering signal and thus affect the accuracy of the retrieval. Microwave emission of a snowpack is related to several properties of the snow cover - particularly, the number of snow particles (snow depth), the size of the grains, and the density of the snowpack. In our project, we are attempting to quantify the uncertainties introduced in the AMSR snow depth retrievals as a result of variations in these and other snowpack properties. The variables studied so far include the effects of surface temperature, ice reflectivity values, correlation length (an approximate measure of grain size), and density on surface microwave emissivities. Specifically, we examined the effects of correlation length and density on the spectral gradient ratio (the basis of the snow depth retrieval algorithm). Followed by an examination of the temporal evolution of the spectral gradient ratio for a multi-layered snowpack with and without an icy layer in section. Below, we describe results of these error and sensitivity analyses and conclude with an initial comparison of simulated and observed snow conditions during AMSRIce03.

Main findings from the modeling studies to date include:

- Emissivity increases with increasing surface temperature, while sensitivity to the surface temperature grows with increasing frequency.
- Relative to other factors, emissivity sensitivity to surface temperature is very small and can be ignored.
- The emissivities for all frequencies, except the 18 GHz horizontal channel, are more sensitive to snow depth change at larger grain sizes and smaller densities.
- The emissivities for all frequencies are more sensitive to grain size and density variation at larger snow depths.
- The effect of densification on the ratio of 18 GHz V and 37 GHz V (gradient ratio) is to increase the ratio positively (towards zero) while correlation length growth increases it negatively.
- Correlation length growth dominates the densification process in the microwave signal.
- The 89 GHz emissivity may be used to detect new snow fall evolution.

- The gradient ratio of 18 GHz and a lower frequency channel (6 or 10 GHz) may be used to retrieve depths of older, deeper snow pack where the gradient ratio at 37 and 18 GHz saturates.
- Horizontal emissivities are more sensitive to icy layers in the snowpack than are vertical channels.
- Comparisons of simulated gradient ratio to observed snow depth along the Ice Camp Line show good agreement, confirming the sensitivity of GR to variations in snow depth.

An overview of a selection of these experiments are given below. Full details can be found in Powell et al. (2004).

3.1 Effects of Different Underlying Ice Thicknesses

A single layer MEMLS simulation was run, changing sea ice reflectivities for the 6, 18, 37, and 89 GHz horizontal and vertical polarizations. In this case, the reflectivities are derived from emissivities reported in the literature for different sea ice thicknesses. Snow depth was then varied from 10 to 90cm over each of these ice conditions.

Figure 14 shows results from this experiment, depicting the effects on emissivity of snow depth at horizontal and vertical emissivity for the different ice reflectivities (ice types). Gray nilas has the highest reflectivity (in the microwave frequencies), while first-year ice and light nilas follow. The most obvious features are that the 89 GHz channel is largely unaffected by the parameterization of the ice reflectivity and that the 6 GHz channel is the most affected frequency.

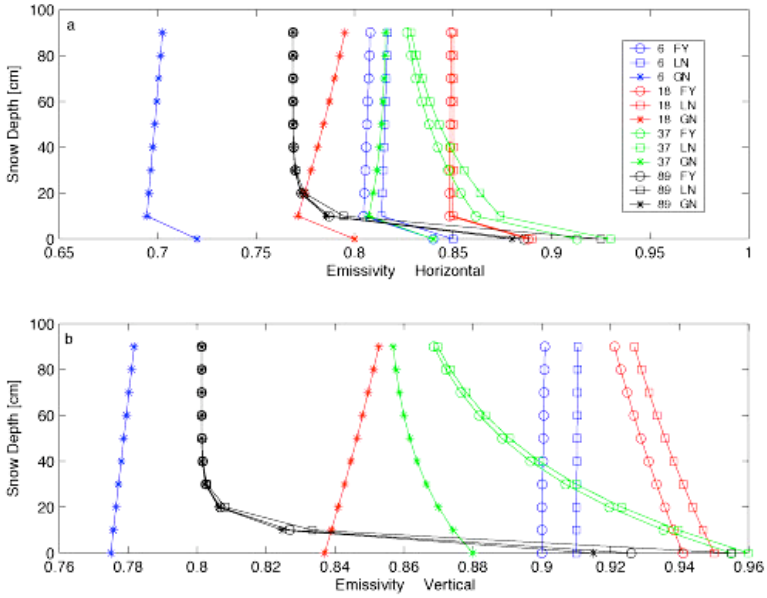

Figure 14. Effects of combinations of ice thickness (ice type) and snow depth on simulated emissivities.

The shallow penetration depth of the 89 GHz channel results in a reduced effect of ice reflectivity on the emissivity for snow depths >10cm while the opposite is true for 6 GHz. Also, the 37 GHz channel's emissivities converge due to a reduced effect of ice reflection on emissivity for deep snow. In both the vertical and horizontal polarizations, the gray nilas has the lowest emissivities due to it's higher ice reflectivity. The first year ice and light nilas reflectivities do not differ greatly in emissivity, although the first-year ice reflectivities result in slightly lower emissivities.

3.2 Snow Temperature Effects

MEMLS simulations were run beginning with a surface temperature of 240K, increasing in increments of 1K. Although the physical properties of the snow cover were kept constant in this experiment, we used 10 layers in order to account for the temperature gradient within the snow. The snow depth was 30 cm.

For all frequencies, the emissivity increases with increasing surface temperature. The effect on emissivity of different surface temperatures grows stronger with increasing frequency so that the maximum change in emissivity is for the 89 GHz vertical polarization channel. This is a small change in emissivity (0.0759) over the 40K range in temperatures relative to the effects of other snow pack properties (see below). Thus, the 6, 18, and 37 GHz channels are relatively insensitive to changes in the surface temperature.

3.3 Effects of Grain Size

Single layer MEMLS simulations were run varying the correlation length from c=0.03mm to c=0.30mm. For each correlation length, the snow depth was changed from 5 to 90 cm. Figure 15 shows results of this experiment. Results are given for 6 GHz (blue lines), 18 GHz (red lines), 37 GHz (green lines), and 89 GHz (black lines). The different correlation lengths used for this simulation set are 0.03 mm (circles), 0.12 mm (squares), 0.21 mm (stars), and 0.30 mm (triangles).

Overall, the emissivities for the microwave frequencies decrease with increasing correlation length. This effect is stronger with increasing frequency. The rate of change of the emissivities increases as correlation length increases (correlation length and emissivity have a non-linear relationship). The correlation length also affects the sensitivity of the emissivities to snow depth. Emissivities decrease with increasing snow depth for most correlation lengths and frequencies (adding snow adds more scatterers, reducing the emission). For very small correlation lengths (<0.12mm), the emissivities increase with increasing snow depth. The smaller particles are less efficient scatterers of microwave radiation than the larger particles and thus rather than adding more scatterers and reducing the emission by increasing the snow depth, emitters are added producing higher emissivities.

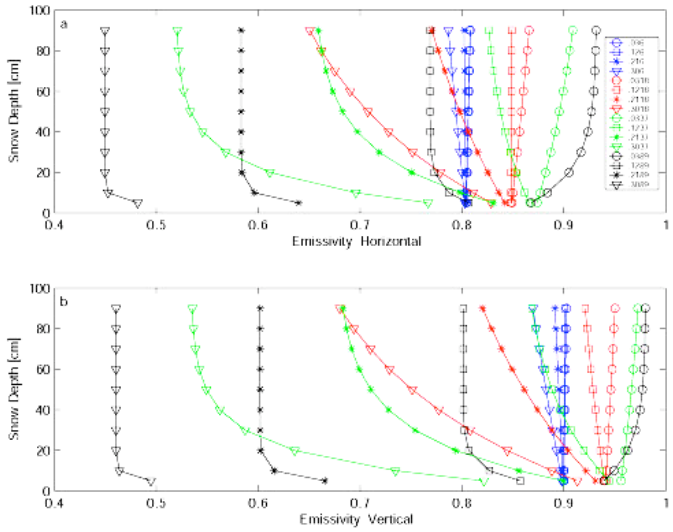

Figure 15. Effects of correlation length on emissivity as a function of snow depth.

3.4 Snow Density Effects

Single layer MEMLS simulations were run, varying the snow pack density from 100 to 400 kg/m^3. For each density the snow depth was changed from 5 to 90 cm. Figure 16 illustrates the impact of snow depth and density on emissivity for 6, 18, 37, and 89 GHz in the horizontal and vertical polarizations, respectively. The densities included are 100 kg/m3 (circles), 200 kg/m3 (squares), 300 kg/m3, and 400 kg/m3 (triangles).

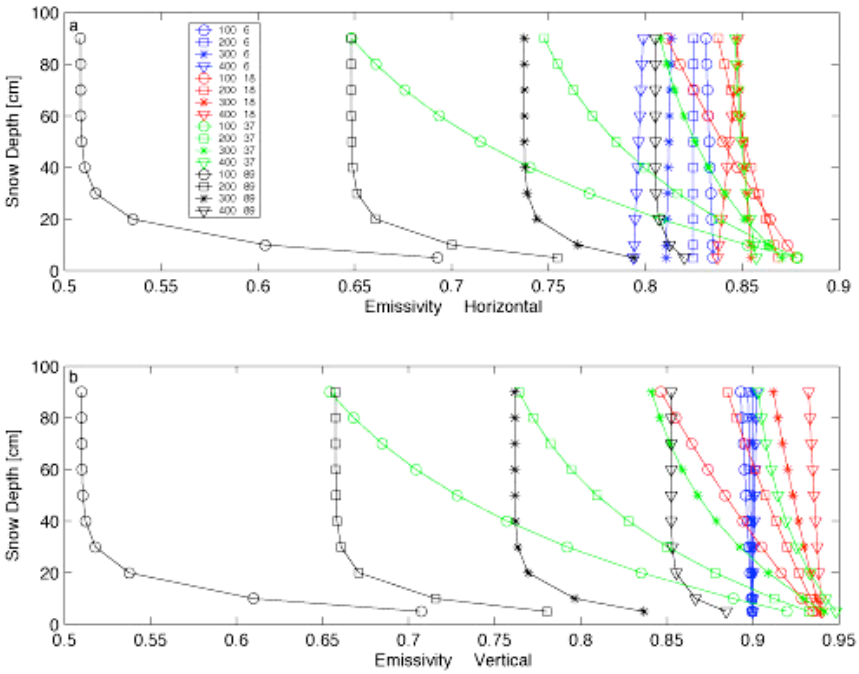

Figure 16. Effects of snow density on emissivity as a function of snow depth.

As density increases the microwave emissivities increase for all frequencies in the vertical polarization and for a majority in the horizontal polarization. The exceptions are the 6 GHz channel, which decreases in horizontal emissivity with increasing density, and the 18 and 37 GHz channels. The 89 GHz channel is the most sensitive to density change in both the horizontal and vertical polarizations relative to the other frequencies.

Density affects the sensitivity of the emissivities to snow depth in much the same way that correlation length does. Large densities correspond to small correlation lengths while smaller densities correspond to larger correlation lengths in their effects on emissivity sensitivity to snow depth. For example, as snow depth increases, the 18 GHz horizontal emissivity increases for a density of 400 kg/m3. This was the case for very small correlation lengths. At all other densities the emissivity decreases with increasing snow depth.

3.5 Simulations Using AMSRIce03 *In situ* Data

As noted in Section 1, the next step in our modeling strategy is to do microwave emission simulations using *in situ* data as model forcings, and then compare these results to the PSR data. Figure 17 shows results of such a simulation using information from the Ice Camp site. As in the sensitivity analyses above, MEMLS is used to simulate emission from snow. In this experiment, ice emissivities were supplied in two ways – by MWMOD runs and by prescribing emissivities based on observations in the literature. In this case, the *in situ* data were collected over multiyear ice, so the emissivities of the underlying ice were modeled (via MWMOD) and prescribed to be values appropriate for multiyear ice. The simulation shown here suggests that for the relatively deep snowpacks at this location, emission from the snowcover may be dominating the gradient ratio signal, masking that of the underlying ice.

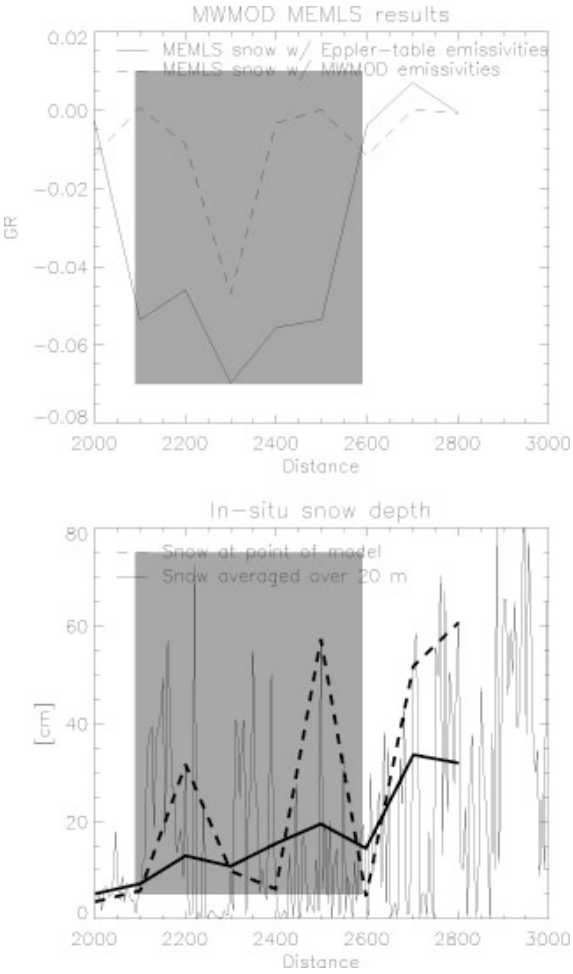

Figure 17. Forward-model (MEMLS + MWMOD) simulations of spectral gradient ratio using *in situ* data as model input for locations along the Ice Camp line.

4.0 Supporting Activities

In addition to the data collection, analysis and modeling activities described above, considerable effort was expended in Year 2 on various image data acquisition and processing activities. These included collection and georeferencing of RADARSAT SAR imagery during the AMSRIce03 period, assembling a basic geographic information system for the AMSRIce03 field data (e.g., Figures 18 and 19), and carrying out various other data archiving tasks. All data sets are being referenced to the polar stereographic "SSM/I grid" to facilitate comparison with AMSR-E imagery. Additional activities included updating of the project web page (http://polarbear.colorado.edu/AMSRIce03), preparation of conference abstracts, and presentations at science team meetings.

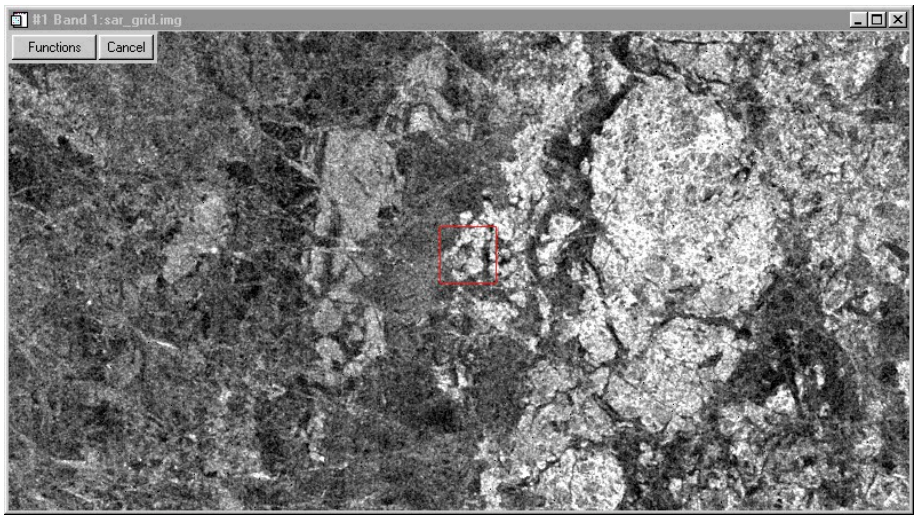

Figure 18. Example of one of many RADARSAT SAR images acquired during Year 2 that have been georeferenced and added to a geographic information system to support data access and processing. The area indicated by the red box is the location of the Navy ice camp area on 19 March 2003.

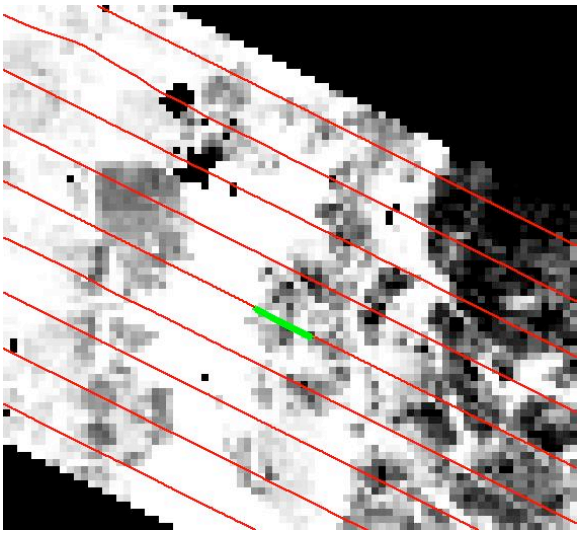

Figure 19. An example of georeferencing of aircraft with other image data (in this case, RADARSAT SAR). The P-3 flight lines are shown in red. The green line shows the location of the Ice Camp transect. Note the good match between the *in situ* transect and the overlying P-3 flight line. The different gray tones relate primarily to ice type – first-year ice is brighter, with multiyear ice shown in darker gray shades.

Figure 20 illustrates the utility of these various georeferenced data sets for validation comparisons underway by T. Markus and collaborator, D. Cavalieri, using our data sets. The mosaics of individual PSR channel data in Figure 20 show good correspondence

with the ice types seen in the SAR image portion in Figure 19. Both image data sets agree with the *in situ* observations regarding ice conditions in this location.

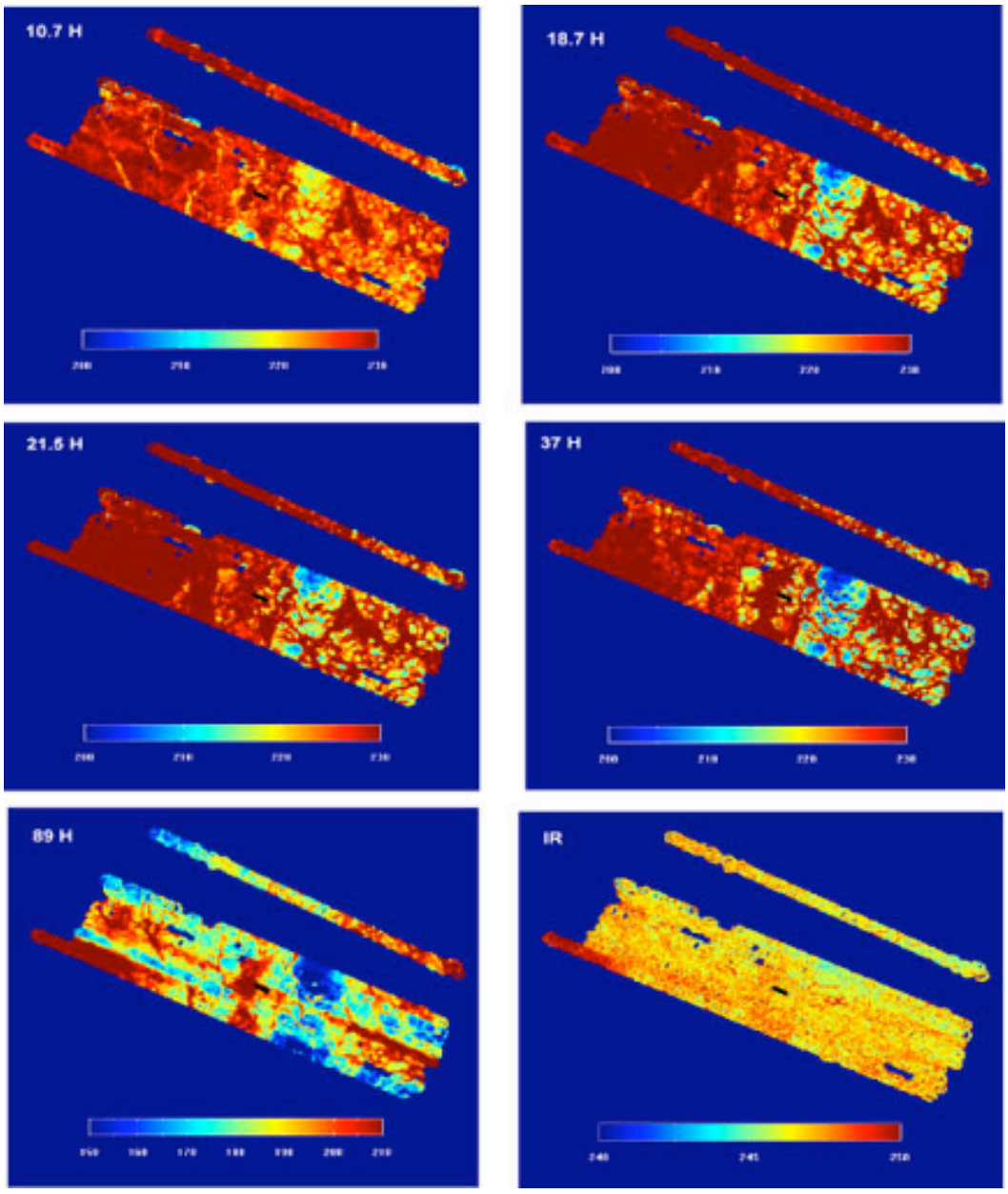

Figure 20. Mosaics of image data acquired over the ice camp location on 19 March 2003 by the NASA P-3. Shown here are the PSR horizontally-polarized microwave channels and thermal infrared data (lower right panel).

5.0 Plans

All the activities described above have been done with one goal in mind – to provide us with the data sets and tools needed for validation of the AMSR-E sea ice products. The effort to date has now brought us to the point where direct comparisons and modeling studies can begin in earnest. Plans for remaining work therefore include:

- Completion of summaries, documentation and archival of AMSRIce03 data.
- Comparison of PSR-derived (simulated AMSR-E) sea ice products with *in situ* data sets to quantify errors and identify main sources of error.
- Generation of MEMLS/MWMOD simulations with *in situ* data as input.
- Refinement of MEMLS/MWMOD through comparison to PSR data.
- Assembly of model simulations in a "2-D" mode to produce simulated radiances along each *in situ* transect and comparison to PSR data.
- Generation of simulations of AMSR-E products and quantification of errors over other ice and atmospheric conditions.
- Analysis, through observations and modeling, of the dominant factors influencing observed microwave emissions at aircraft and satellite altitudes.

6.0 References

Fuhrhop, R., C. Simmer, M. Schrader, G. Heygster, K-P. Johnsen, P. Schussel, 1997. Study of Passive Remote Sensing of the Atmosphere and the Surface Ice: Executive Summary and Final Report, ESA ESTEC Contract No.11198/94/NL/CN, Berichte IfM Kiel, Nr. 29

Maetzler, C., Relation between grain size and correlation length of snow, *J. Glaciol.*, 2002 (in press).

Markus, T. and D.J. Cavalieri, Snow depth distribution over sea ice in the Southern Ocean from satellite passive microwave data, in Antarctic Sea Ice Physical Processes, Interactions and Variability, *Antarctic Research Series, 74*, edited by M.O. Jeffries, pp.19-40, AGU, Washington, D.C., 1998.

Powell, D.C., T. Markus, J.A. Maslanik, 2004. Sensitivites of passive microwave snow depth retrievals to changes in snow physical properties using radiative transfer calculations, (in prep.)

Wiesmann, A., and C. Maetzler, Documentation for MEMLS 98.1, *Research Report No. 98-2,* 22pp., University of Bern, Switzerland, 1998.

Wiesmann, A., and C. Maetzler, Microwave Emission Model of Layered Snowpacks, *Rem. Sens. Env., 70,* 307-316, 1999.

Table 1. Participants in the AMSRIce03 field experiment.

P-3B Aircraft Participants	Affiliation
Donald J. Cavalieri	NASA Goddard Space Flight Center
Thorsten Markus	NASA Goddard Space Flight Center
Albin J. Gasiewski	NOAA/Environmental Technology Laboratory
Vladimir Irisov	NOAA/Environmental Technology Laboratory
Marian Klein	NOAA/Environmental Technology Laboratory
John Barrick	NASA Langley Research Center
Lee Thornhill	NASA Langley Research Center
Dave Easmunt	NASA Wallops Flight Facility
Mike Singer	NASA Wallops Flight Facility
Rich Rogers	NASA Wallops Flight Facility
George Postell	NASA Wallops Flight Facility
John Sonntag	NASA Wallops Flight Facility
Rob Russel	NASA Wallops Flight Facility
Richard Mitchel	NASA Wallops Flight Facility
John Scott	NASA Wallops Flight Facility
Jeff Andrews	National/Navy Ice Center
William P. McAnallen	National/Navy Ice Center
Bernard Walter	NorthWest Research Associates
Sinead L. Farrell	University College, London UK

Surface-Based Participants	Affiliation
James Maslanik	University of Colorado, Boulder
Matthew Sturm	CRREL, AK
Julienne Stroeve	University of Colorado, Boulder
John Heinrichs	Fort Hays State Univ., KS
Jon Holmgren	CRREL, AK
John Govonni	CRREL, AK
Jackie Richter-Menge	CRREL, NH
Don Perovich	CRREL, NH
Paquita Zuidema	NOAA ETL

Cessna 185 Aerial Reconnaissance	Affiliation
Tom George	Terraterpret, Inc.